

# How Dynamic Hydrophobicity of Superhydrophobic Surfaces Governs Evaporation of Small Water Droplets

S.A. Kulinich and M. Farzaneh

NSERC / Hydro-Quebec / UQAC Industrial Chair on Atmospheric Icing of Power Network Equipment (CIGELE) and  
Canada Research Chair on Engineering of Power Network Atmospheric Icing (INGIVRE) <http://cigele.ca>  
at Université du Québec à Chicoutimi, Chicoutimi, QC, Canada

**Abstract—** Recently, the dynamic hydrophobicity (which is described by wetting hysteresis) of surfaces has been investigated extensively. In this work, we experimentally analyze how water droplets evaporate on rough superhydrophobic surfaces (i.e. with water contact angle values over  $150^\circ$ ). We show that small water droplets demonstrate different evaporation modes on superhydrophobic polymer surfaces with the same chemistry but different hysteresis of contact angles. While on the high-hysteresis surface, evaporation follows the constant-contact-diameter mode, whereas the constant-contact-angle mode dominates on the low-hysteresis surface. These modes were previously reported for smooth hydrophilic and hydrophobic surfaces, respectively. Moreover, the lifetime of the droplets on a low-hysteresis surface is always longer than that on a high-hysteresis one. Thus, this study demonstrates the crucial role that surface dynamic hydrophobicity plays in the evaporation behavior of small droplets placed on rough superhydrophobic surfaces.

**Keywords:** Superhydrophobicity; Roughness; Water contact angle; Wetting hysteresis; Evaporation

## I. INTRODUCTION

Recently, superhydrophobic surfaces, i.e. those exhibiting water contact angles (CAs) over  $150^\circ$ , have attracted significant interest [1,2]. Such surfaces are attractive for a variety of applications from anti-sticking, anti-contamination and self-cleaning to anti-corrosive, frost- and snow-repellent, low-friction coatings, among others [1-5]. In parallel, studies on the dynamic behavior of such surfaces have been attracting more and more interest [1,4,6-9]. This can be explained by the belief that static hydrophobicity alone is not sufficient to fully characterize the wetting properties of surfaces [4,6-9]. Free evaporation of small water droplets from various surfaces is an apparently simple problem related to the dynamic behavior of such systems, with relevance to both academic and practical interests. However, more complete knowledge of how evaporation influences the CA and water drop shape is still necessary for better understanding numerous dynamic wetting/dewetting processes involved on surfaces. That knowledge is also very important in wetting and surface characterization processes since CA (as an important parameter characterizing surface properties) appears to change when inevitable evaporation of water in air occurs.

While extensive studies have been carried out on the evaporation of water droplets from solids [11-17], relatively little research has been done on hydrophobic surfaces [14-16,18], and even less so on superhydrophobic surfaces [13,16,19]. McHale and co-workers studied evaporation on a superhydrophobic surface formed by patterned polymer and having high CA hysteresis (CAH) [16]. It was shown that water droplets initially evaporated in a pinned contact line (so called constant-contact-diameter, CD) mode, before the contact line receded in a stepwise fashion, jumping from pillar to pillar of the patterned surfaces [16]. An abrupt collapse of some droplets into the pillar structure was observed in some cases during evaporation, while other droplets appeared to collapse into the structure only at very late stages of evaporation, which could not be detected by the optics used [16]. Zhang et al. [13] followed sessile water droplets evaporating on superhydrophobic lotus leaf and biomimetic polymer surfaces. Both hierarchically-structured samples demonstrated the constant-CD mode of evaporation, while CAH values were not evaluated. Evaporation on super water-repellent surfaces with low CAH has not been reported up to date.

It is well accepted in the literature that there are two conditions, in the case of a small water drop, determining the behavior of both CA and CD during its major stage of evaporation from a smooth surface [14,18,20]. More specifically, on wetting solids with  $CA < 90^\circ$ , the evaporation rate was reported to be linear with time, with CA decreasing and CD remaining constant (the constant-CD mode) [15,17,18,20]. On non-wetting solids, the rate of evaporation was found to be non-linear, since CA remains constant, while CD decreases (the constant-CA mode) [14,18]. It was suggested that CAH is a factor influencing drop evaporation, in particular on rough surfaces [12,15,18,21], but no systematic work has been conducted so far to elucidate its effect. In this study, the evaporation of sessile drops on superhydrophobic surfaces with  $CA > 150^\circ$  is investigated. The importance of the dynamic hydrophobicity of the surface as another parameter governing evaporation (which is itself a dynamic event) is demonstrated. It is shown that depending on a large or small value of CAH, the dominant stage of the evaporation can follow either constant-CD or constant-CA modes, as previously mentioned for wetting or non-wetting systems, respectively.

## II. EXPERIMENT

The samples were prepared on aluminum plates ( $2.5 \times 2.5 \text{ cm}^2$ ) which were polished with emery paper and cleaned in organic solvents.  $\text{ZrO}_2$  nanopowder (3.0 g) with an average size of 20-30 nm from Aldrich was mixed with 40 ml of deionized water. The suspension was sonicated for 30 min, after which 2.4 ml of a perfluoroalkyl methacrylic copolymer (Zonyl 8740, DuPont) product were added. The final suspension was stirred for another 3 h before coating on the substrates. The superhydrophobic sample A was prepared by uniformly spraying the suspension over the substrate surface and letting it dry at  $\sim 50^\circ\text{C}$ . The superhydrophobic sample B was prepared by spin-coating of the same suspension on the substrate. Upon coating, the samples were heat-treated at  $120^\circ\text{C}$  in air for 3 h to remove the residual solvents.

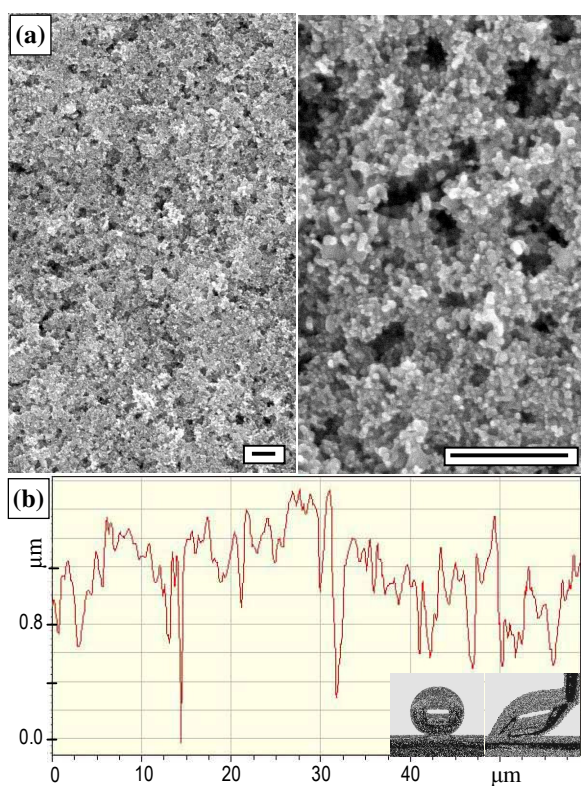


Fig. 1. Surface images of sample A at different magnification (a) and surface profile (b). Sessile and moving (with a needle) water droplets ( $4 \mu\text{L}$ ) are shown as insets. CA value is  $152.1^\circ \pm 3.5^\circ$ , CAH value is  $> 70^\circ$ . Scale bars indicate 500 nm.

CA and CAH values were measured by following standard protocols on a Krüss DSA10 contact-angle goniometer; the values reported herein were the average of at least five measurements on various parts of each sample. They were recorded at  $23 \pm 0.5^\circ\text{C}$  with distilled water; all droplets were  $4 \mu\text{L}$  in volume. The same instrument was used to observe water droplet evolution over time as a result of evaporation. Long-term behavior of water drops on the surfaces was evaluated by measuring the evolution of their contact angle and contact diameter on each surface for periods of time up to  $\sim 43$  min (until the droplets could be detected by

the optics). Several droplets were observed during their evaporation on each sample, showing good statistical consistency. The evaporation curves presented below were chosen as typical for each sample.

Advancing contact angles were measured after sequential deposition with a small syringe and needle. A small drop was deposited on the surface, and then additional water was added to advance the contact line. The needle was inserted into the drop during injection to prevent drops from moving on the super water-repellent surface B. For receding contact angles, water was withdrawn until the contact line retracted. Measurements were made on both sides of more than five droplets and then averaged. Scanning electron microscopy (SEM) of the sample surfaces was carried out with a JSM-6330-F microscope (JEOL) after coating them with a thin conducting layer of Pt. Topography of the sample surfaces was analyzed with a WYKO NT1100 optical profilometer (Veeco). X-ray photoelectron spectroscopy (XPS) was performed with a Quantum-2000 instrument from ULVAC-PHI.

## III. RESULTS AND DISCUSSION

Several sources of wetting hysteresis are normally recognised in the literature. Among those, the major ones are considered to be either chemical (e.g. nonhomogeneity of chemical composition of the solid surface) or physical (of which roughness is probably the most known) [19,20,22,23]. Therefore, to prepare superhydrophobic surfaces with different CAH, the roughness of the samples was varied by depositing fluoropolymer coatings, incorporated with  $\text{ZnO}_2$  nanoparticles, either by spraying (sample A) or by spin-coating (sample B). This led to different surface roughness and CAH characteristics of the samples (see Figs. 1 and 2). Both samples exhibit superhydrophobic properties with very close CA values in the range of  $\sim 152$ - $153^\circ$ . At the same time, as seen in Figs. 1b and 2b (insets), the CAH values of the samples are very different, being  $> 70^\circ$  and  $\sim 5^\circ$  for samples A and B, respectively. Thus, of the two samples prepared, one demonstrates a “sticky” state (A) and the other “slippy” state (B) for water droplets on their surfaces [1,22]. As seen from the SEM images in Fig. 1a, asperities are less separated and have larger surface area in sample A, with their tops being relatively flat and shallow. Therefore, water drops are expected to have larger water-solid contact area on this surface, leading to the high CAH and “sticky” state [22,23] observed in Fig. 1b (inset). Meanwhile, sharper and better separated asperities are observed in the SEM surface images of sample B (Fig. 2a), which is normally associated with lower CAH and “slippy” state of superhydrophobic surfaces [22,23]. Comparison of surface profiles of the samples (Figs. 1b and 2b) also confirms that the asperities in sample B are better separated and higher, giving rise to larger surface roughness. The root-mean-square roughness value of sample B was evaluated by optical profilometry to be  $\sim 419$  nm, which is larger than that of sample A ( $\sim 257$  nm).

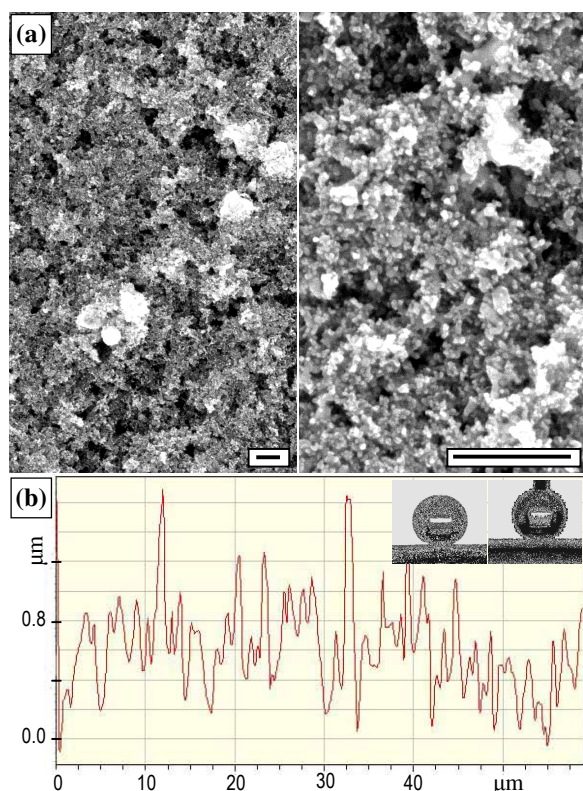


Fig. 2. Surface images at different magnification (a) and surface profile (b) of sample B. Sessile and moving (with a needle) water droplets ( $4 \mu\text{L}$ ) are shown as insets. CA value is  $153.3^\circ \pm 1.5^\circ$ , CAH value is  $4.9^\circ \pm 1.7^\circ$ . Scale bars indicate 500 nm.

Since both samples exhibit  $\text{CA} > 150^\circ$ , it is safe to conclude that oxide nanoparticles only contribute to surface roughness, while it is the fluoropolymer that is in the topmost layer all over the surface. That is, both samples have similar surface chemistry, and it is their surface roughness that is responsible for the difference in dynamic hydrophobicity observed. This is supported by XPS analysis (results not shown here), as only F, Zr, C, O and Al peaks were seen in both XPS survey spectra. The atomic ratio of the elements present in the coatings, F:Zr:C:O, was equal to 1.2:0.91:10.09:4.83 and 1.24:1.01:11.93: 5.35 for samples A and B, respectively.

Figure 3 compares changes in CA (a) and CD (b) for two droplets as they evaporate on samples A and B. Figure 4 shows photographs of the same droplets corresponding to evaporation times of 32, 34, 36, and 38 min. As seen in Fig.3a, the initial values of CA were both slightly greater than  $150^\circ$ , and the corresponding values of CD in Fig.3b were also very close, being about 0.92 and 0.86 mm for samples A and B, respectively. Thus, the initial geometric parameters of the droplets, related to the static hydrophobicity of the surfaces, were comparable.

The CA of the droplet on surface A is seen to steadily decrease over time in Fig.3a, while its CD remains approximately constant up to  $\sim 2250$  s (when CD is observed

to be  $\sim 0.77$  mm). After this, a fast decrease in CD is observed till  $\sim 2300$  s, when the last measurement on sample A was possible, resulting in a CD value of about 0.6 mm, as shown in Fig.3b. In contrast, the droplet on surface B exhibits a smooth decrease in its CD, and the last measurement at  $\sim 2600$  s gives a CD value as small as 0.06 mm, which is about one order of magnitude lower than that observed on sample A (see Fig.3b). In agreement with the typical constant-CA mode observed on hydrophobic surfaces by others [14,18], a quasi-static CA – time dependence is observed up to  $\sim 2500$  s for sample B, as seen in Fig.3a, after which a steep slope is observed with the last measurement at  $\sim 2600$  s showing  $\text{CA} \sim 90^\circ$  (Fig.4b, inset). The evaporation on sample A ends after  $\sim 2300$  s, when the last CA observed is lower than  $10^\circ$  (see Fig.4d). Note that time dependencies similar to those in Figs.3a,b have been observed for all droplets studied.

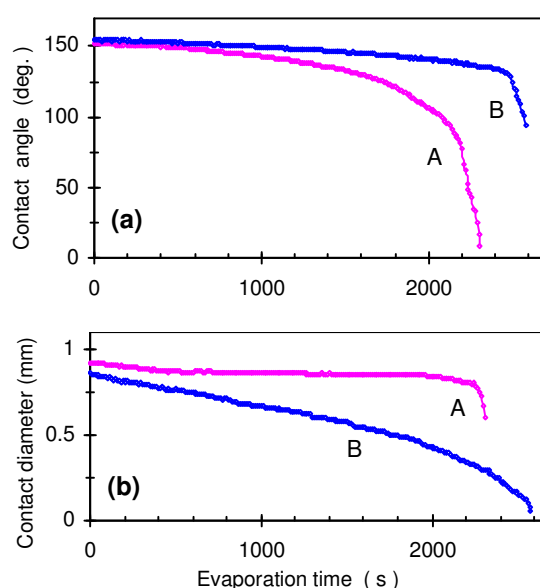


Fig. 3. Evolution of contact angle (a) and contact diameter (b) of water droplets ( $4 \mu\text{L}$ ) evaporating on surfaces A and B.

All the above peculiarities of the dynamic behavior of water drops on the high-CAH surface A appear to be related to its high “sticky” ability. As the contact line is not mobile and tends to be pinned on this surface, it must be accompanied by a reduction in CA when evaporation proceeds, as clearly shown in Figs.4a-d. This contrasts sharply the behavior of the droplets on the low-CAH surface B, where the contact line is very mobile ( $\text{CAH} \sim 5^\circ$ ) so that it moves quickly as evaporation proceeds and droplet volume goes down (Figs.4e-h). This contact line motion without pinning on surface heterogeneities is believed to sustain the observed quasi-static CA evaporation as the dominating mode on sample B. It is clearly seen in Figs.3,4 that even just a few seconds before its disappearance, the droplet on sample A is much pinned down and exhibits very low CA, whereas the one on sample B has a much smaller contact area and higher CA.

Furthermore, the difference in the contact line motion (pinned or mobile behavior) appears to be responsible for the different life-times of the droplets observed in Fig.3. As the CA of the pinned droplet (Fig.3a, curve A) approaches  $90^\circ$ , and eventually drops below this value (Fig.4b), evaporation through the entire water-air interface must become possible as a shape of a droplet with  $CA < 90^\circ$  cannot hinder any air circulation near the contact line any longer [14]. Therefore, as the shape of drop A gradually turns into that with  $CA < 90^\circ$ , the droplet mass loss must increase if compared to that of drop B, which essentially keeps its CA above  $90^\circ$  all the time (see Fig.3a, curve B). This inevitably leads to the shorter life-time of drop A. The photographs in Fig.4 are well consistent with the above explanation. Indeed, while droplets in Figs.4a,e (after evaporation for 32 min) appear to be comparable in terms of their volume, a big mass loss is observed between 34 and 38 min (Figs.4b-d), when the droplet on the high-CAH surface has reached CA values  $< 90^\circ$ . At the same time, the volume change between 34 and 38 min in Figs.4f-h is obviously smaller, thus confirming a slower evaporation rate from the lower part of the droplet which holds its  $CA > 90^\circ$  on sample B.

fact that high values of  $CA > 90^\circ$  are sustained on the low-hysteresis surface for much longer periods of time, and the evaporation rate of such droplets is likely to be suppressed in the area close to the contact line. Local saturation vapor is generated near the contact line which hinders evaporation. In contrast, drops on the high-hysteresis surface reached values of  $CA < 90^\circ$  faster, from which point in time evaporation takes place from the entire water-air interface.

## V. ACKNOWLEDGMENTS

This work was carried out within the framework of the NSERC/Hydro-Quebec/ UQAC Industrial Chair on Atmospheric Icing of Power Network Equipment (CIGELE) and the Canada Research Chair on Engineering of Power Network Atmospheric Icing (INGIVRE) at Université du Québec à Chicoutimi. The authors would like to thank the CIGELE partners (Hydro-Quebec, Hydro One, Réseau Transport d'Électricité (RTE) and Électricité de France (EDF), Alcan Cable, K-Line Insulators, Tyco Electronics, Dual-ADE, and FUQAC) whose financial support made this research possible.

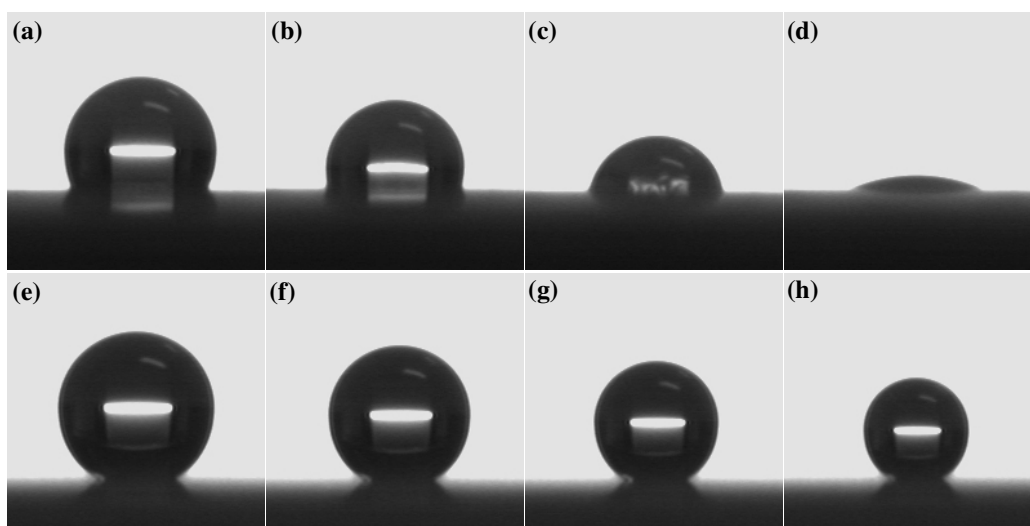


Fig. 4. Drop photographs on superhydrophobic surfaces A (a-d) and B (e-h); evaporation times are 32 (a,e), 34 (b,f), 36 (c,g) and 38 (d,h) min; faster evaporation is observed between (b) and (d) compared to (f) through (h).

## IV. CONCLUSIONS

In conclusion, the evaporation of small water droplets on superhydrophobic surfaces ( $CA > 150^\circ$ ) with similar surface chemistry has been shown to follow different modes, depending on the dynamic hydrophobicity of the surfaces. More specifically, the surface with a low CAH was observed to follow the evaporation model normally ascribed to hydrophobic surfaces (quasi-static CA while constantly decreasing CD for most of the evaporation time). Meanwhile, the surface with a high CAH was found to behave in accordance with the evaporation model normally associated with hydrophilic surfaces (constantly decreasing CA and quasi-static CD). Water droplets were observed to evaporate faster on the surface with high CAH. This is attributed to the

## VI. REFERENCES

- [1] X.M. Li, D. Reinhoudt, and M. Crego-Calama, "What do we need for a superhydrophobic surface? A review on the recent progress in the preparation of superhydrophobic surfaces," *Chem. Soc. Rev.*, vol.36, pp.1350-1368, 2007.
- [2] A. Nakajima, K. Hashimoto, and T. Watanabe, "Recent studies on superhydrophobic films," *Monatsh. Chem.*, vol.132, pp.31-41, 2001.
- [3] H. Wang, L.M. Tang, X.M. Wu, W.T. Dai, and Y.P. Qiu, "Fabrication and anti-frosting performance of super hydrophobic coating based on modified nano-sized calcium carbonate and ordinary polyacrylate," *Appl. Surf. Sci.*, vol.253, pp.8818-8824, 2007.
- [4] S.A. Kulinich and M. Farzaneh, "Alkylsilane self-assembled monolayers: Modeling their wetting characteristics," *Appl. Surf. Sci.*, vol.230, pp.232-240, 2004.
- [5] A. Nakajima, "Design of a transparent hydrophobic coating," *J. Ceram. Soc. Jpn.*, vol.112, pp.533-540, 2004.

- [6] D. Öner and T.J. McCarthy, "Ultrahydrophobic surfaces. Effects of topography length scales on wettability," *Langmuir*, vol.16, pp.7777-7782, 2000.
- [7] S.A. Kulinich and M. Farzaneh, "On wetting behavior of fluorocarbon coatings with various chemical and roughness characteristics," *Vacuum*, vol.79, pp.255-264, 2005.
- [8] W. Chen, A.Y. Fadeev, M.C. Hsieh, D. Öner, J. Youngblood, and T.J. McCarthy, "Ultrahydrophobic and ultralyophobic surfaces: some comments and examples," *Langmuir*, vol.15, pp.3395-3399, 1999.
- [9] M. Miwa, A. Nakajima, A. Fujishima, K. Hashimoto, and T. Watanabe, "Effects of the surface roughness on sliding angles of water droplets on superhydrophobic surfaces," *Langmuir*, vol.16, pp.5754-5760, 2000.
- [10] J.-H. Song, M. Sakai, N. Yoshida, S. Suzuki, Y. Kameshima, and A. Nakajima, "Dynamic hydrophobicity of water droplets on the line-patterned hydrophobic surfaces," *Surf. Sci.*, vol.600, pp. 2711-2717, 2006.
- [11] R.G. Picknett and R. Bexon, "The evaporation of sessile or pendant drops in still air", *J. Colloid. Interf. Sci.*, vol.61, pp.336-350, 1977.
- [12] H.-Z. Yu, D.M. Soolaman, A.W. Rowe, and J.T. Banks, "Evaporation of water microdroplets on self-assembled monolayers: from pinning to shrinking", *ChemPhysChem*, vol.5, pp.1035-1038, 2004.
- [13] X.Y. Zhang, S.X. Tan, N. Zhao, X.L. Guo, X.L. Zhang, Y.J. Zhang, and J. Xu, "Evaporation of sessile water droplets on superhydrophobic natural lotus and biomimetic polymer surfaces", *ChemPhysChem*, vol.7, pp.2067-2070, 2006.
- [14] G. McHale, S.M. Rowan, M.I. Newton, and M.K. Banerjee, "Evaporation and the wetting of a low-energy solid surface", *J. Phys. Chem. B*, vol.102, pp.1964-1967, 1998.
- [15] C. Bourgès-Monnier and M.E.R. Shanahan, "Influence of evaporation on contact angle", *Langmuir*, vol.11, pp.2820-2829, 1995.
- [16] G. McHale, S. Aqil, N.J. Shirtcliffe, M.I. Newton, and H.Y. Erbil, "Analysis of droplet evaporation on a superhydrophobic surface", *Langmuir*, vol.21, pp.11053-11060, 2005.
- [17] S.M. Rowan, M.I. Newton, and G. McHale, "Evaporation of microdroplets and the wetting of solid surfaces", *J. Phys. Chem.*, vol.99, pp.13268-13271, 1995.
- [18] K.S. Birdi and D.T. Vu, "Wettability and the evaporation rates of fluids from solid surfaces", *J. Adhes. Sci. Technol.*, vol.7, pp.485-493, 1993.
- [19] M. Reyssat, J.M. Yeomans, and D. Quéré, "Impalement of fakir drops", *Erophys. Lett.*, vol.81, 26006, 2008.
- [20] M.E.R. Shanahan and C. Bourgès, "Effect of evaporation on contact angles on polymer surfaces", *Int. J. Adhes. Adhes.*, vol.14, pp.201-205, 1994.
- [21] H.Y. Erbil, G. McHale, S.M. Rowan, and M.I. Newton, "Determination of the receding contact angle of sessile drops on polymer surfaces by evaporation", *Langmuir*, vol.15, pp.7378-7385, 1999.
- [22] G. McHale, N.J. Shirtcliffe, and M.I. Newton "Contact-angle hysteresis on super-hydrophobic surfaces," *Langmuir*, vol.20, pp.10146-10149, 2004.
- [23] C.W. Extrand, "Model for contact angles and hysteresis on rough and ultraphobic surfaces," *Langmuir*, vol.18, pp.7991-7999, 2002.

Author address: Prof. M. Farzaneh, Chairholder, NSERC/Hydro-Québec/UQAC Industrial Chair on Atmospheric Icing of Power Network Equipment and Canada Research Chair on Engineering of Power Network Atmospheric Icing (INGIVRE), Université du Québec à Chicoutimi 555, Boulevard de l'Université, Chicoutimi, Québec, Canada, G7H 2B1, E-mail: [farzaneh@uqac.ca](mailto:farzaneh@uqac.ca)